



**HAL**  
open science

# A fully scalable 3D non-periodic homogenization method to upscale elastic media

Jian Cao, Romain Brossier, Yann Capdeville, Ludovic Métivier, Serge Sambolian

## ► To cite this version:

Jian Cao, Romain Brossier, Yann Capdeville, Ludovic Métivier, Serge Sambolian. A fully scalable 3D non-periodic homogenization method to upscale elastic media. 84th EAGE Annual Conference & Exhibition, Jun 2023, Vienne, Austria. pp.1-5, 10.3997/2214-4609.202310564 . hal-04278846

**HAL Id: hal-04278846**

**<https://hal.science/hal-04278846>**

Submitted on 10 Nov 2023

**HAL** is a multi-disciplinary open access archive for the deposit and dissemination of scientific research documents, whether they are published or not. The documents may come from teaching and research institutions in France or abroad, or from public or private research centers.

L'archive ouverte pluridisciplinaire **HAL**, est destinée au dépôt et à la diffusion de documents scientifiques de niveau recherche, publiés ou non, émanant des établissements d'enseignement et de recherche français ou étrangers, des laboratoires publics ou privés.

# A fully scalable 3D non-periodic homogenization method to upscale elastic media

J. Cao<sup>1</sup>, R. Brossier<sup>1</sup>, Y. Capdeville<sup>3</sup>, L. Métivier<sup>1,2\*</sup> & S. Sambolian<sup>1</sup>

<sup>1</sup> Univ. Grenoble Alpes, ISTerre, F-38058 Grenoble, France

<sup>2</sup> CNRS, Univ. Grenoble Alpes, LJK, F-38058 Grenoble, France

<sup>3</sup> LPGN, Univ. de Nantes/CNRS, F-44000 Nantes, France

Saturday 21<sup>st</sup> January, 2023

## Main objectives

In this study, we design an efficient and fully scalable parallel algorithm to implement the 3D non-periodic homogenization method for elastic media upscaling, so as to make it easily applicable to seismic full waveform modelling and inversion on large-scale 3D problems.

## New aspects covered

Instead of mathematical proofs and derivations of the homogenization theory, this study is developed from the application point of view. A fully scalable parallel conjugate-gradient iterative scheme is introduced into the 3D non-periodic homogenization process for solving its elastostatic equation systems and applying the low-pass filtering (here we use a cascade of elliptic PDE-defined Bessel filters to approximate the conventional convolution-based Gaussian low-pass filtering without the sacrifice of effectiveness).

## **Summary (200 words)**

Full waveform modelling and inversion are essential tools commonly used in seismic imaging. Due to the restrictions from instruments and computing resources, the seismic data are usually frequency-band limited. Thus, the resulting imaging result is a smooth version of the true Earth with the lack of scales smaller than the minimum propagating wavelength. The non-periodic homogenization technique allows for building a long-wave equivalent medium to account for wave interactions with small geological structures and producing similar waveforms as for the original medium at a controlled accuracy. The current non-periodic homogenization implementation is memory and time consuming even with parallel computing techniques. To boost its applicability on large-scale 3D problems, we propose a fully scalable non-periodic homogenization implementation. As the core of the homogenization process, the solution of elastostatic equations and the low-pass filtering operations are formulated as the linear system solution with a matrix-free conjugate-gradient algorithm to exploit highly optimized matrix-vector-product routines developed in our elastic wave modelling and inversion parallel code SEM46. For the algorithm consistency, an approximated Gaussian low-pass filtering is introduced by a cascade of PDE-defined Bessel filters without sacrificing the effectiveness. All these improvements enhance the efficiency, scalability and robustness of the non-periodic homogenization process.

## A fully scalable 3D non-periodic homogenization method to upscale elastic media

### Introduction

The Earth's interior contains heterogeneities at different scales from macroscopic scales like tectonic units to microscopic scales like pores and mineral grains. However, the seismic waves used in both seismology and oil & gas exploration studies have a limited frequency band because of instrument and computing resource restrictions and intrinsic attenuation properties of the subsurface. It leads to the challenges of how to understand and also account for the heterogeneities that are smaller than the minimum propagating wavelength in seismic imaging. The non-periodic homogenization theory enables the construction of effective density and elastic coefficient models for any elastic media in a long-wavelength asymptotic way, achieving the representation of small-scale heterogeneities/structures with apparent anisotropy to produce similar modelling waveforms as for the original medium at a controlled accuracy (Capdeville et al., 2010; Cupillard and Capdeville, 2018). From the aspect of full waveform inversion (FWI), this theory suggests that the best model retrieved by a limited-frequency FWI is the homogenized version of the true model (Capdeville and Métivier, 2018), which opens the door to physically interpret the FWI reconstructed models and access the true media.

To benefit from the non-periodic homogenization theory in both full waveform modelling and inversion, it is critical to develop an efficient numerical implementation of the homogenization process, especially for its application on large-scale 3D problems. In this study, we consider formulating the non-periodic homogenization method into a parallel conjugate-gradient (CG) iterative scheme based on domain decomposition, which can ensure a good efficiency and scalability on HPC platforms. More precisely, we show the CG iterative algorithm design and optimization for the solution of elastostatic equations and low-pass filtering operations in the homogenization process, respectively. And finally we apply it to two 3D numerical tests for the algorithm evaluation.

### 3D non-periodic homogenization with the conjugate gradient method

The non-periodic homogenization dates back to the computation of effective properties for composite materials in micromechanics (Bensoussan et al., 1978). Its application to seismic wave modelling is derived by Capdeville et al. (2010) and Cupillard and Capdeville (2018) to upscale any 2D and 3D elastic media without size, shape and contrast restrictions on the heterogeneities. In practice, the non-periodic homogenization process is made of three steps:

Step 1: Solve the elastostatic equation with periodic boundary conditions

$$\nabla \cdot \left\{ \mathbf{C} : \left[ \mathbf{I} + \frac{1}{2} (\nabla \boldsymbol{\chi} + \nabla^t \boldsymbol{\chi}) \right] \right\} = \mathbf{0}, \quad (1)$$

where  $\mathbf{I}$  is the 4th-order identity tensor and the solution  $\boldsymbol{\chi}$  is a 3rd-order tensor corresponding to the static response of unit strains. Thanks to the symmetry of the elasticity tensor  $\mathbf{C}$ , Eq. (1) can be written as an equation system with 6 right-hand side vectors ( $\mathbf{b}^{kl} = b_j^{kl} = \partial_i C_{ijkl}$ , with Einstein notation), namely

$$K_{ij} \chi_i^{kl} = -b_j^{kl}, \quad \text{with Einstein notation}, \quad (2)$$

where  $K_{ij}$  is the component form of the stiffness matrix  $\mathbf{K}$ , including the elasticity tensor components  $C_{ijkl}$  and derivative operators,  $\chi_i^{kl}$  is the component form of  $\boldsymbol{\chi}$  and  $kl \rightarrow \beta = 1, 2, \dots, 6$  (Voigt notation).

Step 2: Build the strain and stress concentrators  $\mathbf{G}$  and  $\mathbf{H}$  as

$$\mathbf{G} = \frac{1}{2} (\nabla \boldsymbol{\chi} + \nabla^t \boldsymbol{\chi}) + \mathbf{I}, \quad \mathbf{H} = \mathbf{C} : \mathbf{G}. \quad (3)$$

Step 3: Low-pass filter  $\mathbf{G}$  and  $\mathbf{H}$  to obtain the  $\lambda_0$ -wavelength equivalent effective elasticity tensor  $\mathbf{C}^*$  by

$$\mathbf{C}^* = \mathcal{F}^{\lambda_0}(\mathbf{H}) : \left[ \mathcal{F}^{\lambda_0}(\mathbf{G}) \right]^{-1}. \quad (4)$$

Among these three steps, the implementation of Step 2 is trivial, and therefore we focus on the algorithm design of Steps 1 and 3. In Step 1, we follow the work of Capdeville et al. (2010) and Cupillard and Capdeville (2018) to discretize Eq. (2) with a classic weak-form based spectral-element method (SEM) to match all the strong discontinuities in the media. However, regarding the solution of the resulting discrete system, instead of using a direct solver such as PARDISO or MUMPS, we consider applying a parallel iterative solver that is relatively cheap in terms of complexity and storage and can also overcome the weak scalability and load balancing issues in the state-of-the-art parallel direct solvers (Tang et al., 2022). To guarantee the convergence, we impose homogeneous Dirichlet boundary conditions instead of periodic boundary conditions, and together with the symmetry of elasticity tensor  $\mathbf{C}$ , this makes the stiffness matrix  $\mathbf{K}$  symmetric positive definite. Consequently, this discrete system can be solved by the preconditioned CG method (Hestenes and Stiefel, 1992). Since the boundary condition effect decays

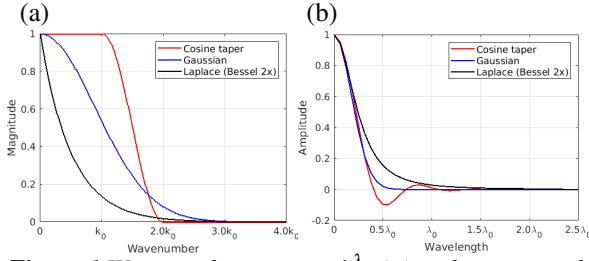


**Figure 1** Wavenumber spectra  $\hat{w}^{\lambda_0}$  (a) and corresponding wavelets  $w^{\lambda_0}$  (b) for three low-pass filters: Cosine-tapered filter, Gaussian filter and Laplace filter implemented by cascading two Bessel filters, with  $2.5\lambda_0$  spatial support.

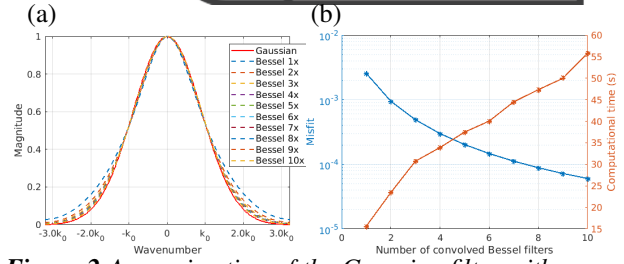


**Figure 2** Approximation of the Gaussian filter with a cascade of Bessel filters (a) and the superposition (b) of the approximation accuracy (blue) and computational cost (orange) with respect to the number of Bessel filters (each one corresponds to a stretching factor  $\alpha$  calculated by PSO).

Model	Size (DOF)	Cores	CG iterations for solving elastostatic equations						CG iterations for low-pass filtering	Elapsed time (s)
			$\mathbf{b}^1$	$\mathbf{b}^2$	$\mathbf{b}^3$	$\mathbf{b}^4$	$\mathbf{b}^5$	$\mathbf{b}^6$		
Random cube	0.81G	960	1514	1500	1531	1508	1510	1509	$\leq 800$	1099
3D Marmousi II	0.63G	960	3403	3440	3437	3482	3703	3320	$\leq 850$	1201

**Table 1** Computational cost for the CG-based iterative homogenization process on two 3D elastic models. Both tests are run on Jean Zay (HPE SGI 8600 supercomputer from IDRIS, CNRS) with Intel Cascade Lake CPU architecture (2.5G Hz, 40 CPU cores per node).

exponentially in the elastostatic equation, the meaningless solutions generated by the homogeneous Dirichlet boundary condition are limited in a thin layer from the boundaries and can be removed by a buffer strategy and the low-pass filtering in Step 3.

As the key of separating the macroscopic and microscopic scales in the homogenization, Step 3 involves the low-pass filtering of concentrators  $\mathcal{F}^{\lambda_0}(\mathbf{G})$  and  $\mathcal{F}^{\lambda_0}(\mathbf{H})$  to remove scales smaller than the wavelength  $\lambda_0$ . Figure 1 shows three available low-pass filters in which the cosine taper filter is closer to the ideal wavenumber response used in the homogenization theory demonstration. The Gaussian filter, however, is widely used in practice because its wavelet is compact and without negative amplitude which would create instability issues during the convolution with highly heterogeneous fields. As mentioned before, we plan to implement the homogenization process within a SEM-based iterative scheme. To keep the algorithm consistency with Step 1 and also avoid extra projection efforts between SEM and Cartesian meshes in the convolution, we promote the use of an elliptic PDE-defined Bessel filter (Trinh et al., 2017)

$$\mathbf{s}(z, x, y) - \left( (\alpha L)^2 \frac{\partial^2}{\partial z^2} + (\alpha L)^2 \frac{\partial^2}{\partial x^2} + (\alpha L)^2 \frac{\partial^2}{\partial y^2} \right) \mathbf{s}(z, x, y) = \mathbf{m}(z, x, y) \quad (5)$$

where  $\mathbf{m}$  is the original vector,  $L$  is the coherent length related to the low-cut wavelength  $\lambda_0$ ,  $\alpha$  is a stretching factor, and the filtered vector  $\mathbf{s}$  can be obtained by solving its resulting SEM-based discrete PDE system with the same CG method used in Step 1. Consequently, the whole homogenization process can be implemented within the same CG iterative scheme with domain decomposition parallelization to achieve the algorithm and accuracy consistency. Thanks to the central limit theorem, Figure 2a shows that the frequency response of the Gaussian filter can be approximated by a cascade of PDE-defined Bessel filters with a well-chosen stretching factor  $\alpha$ . This factor is calculated by solving a wavenumber response fitting problem with the particle swarm optimization (PSO). As expected, increasing the number of Bessel filters yields more accurate approximation of the Gaussian filter. Thus, we consider a trade-off (Bessel 4x with  $\alpha = 6.496\text{E-}2$  or Bessel 5x with  $\alpha = 5.752\text{E-}2$ ) between accuracy and cost by the graph superposition in Figure 2b.

### Numerical examples

To investigate the feasibility of the proposed parallel CG-based homogenization implementation, we run numerical tests on two 3D models with 4th-order SEM mesh on a HPC platform. The detailed computational costs are listed in Table 1, revealing a homogenization problem with unknowns between half and one billion can be solved in less than 20 minutes using 960 CPU cores, thanks to the fast convergence of CG method and excellent scalability of the domain decomposition in our SEM46 code.

For validation, we first homogenize a highly heterogeneous medium incorporating small cubes of  $100\text{m}^3$  with random velocity perturbations in  $\pm 50$  percent of the background properties (Figure 3a). In Figure

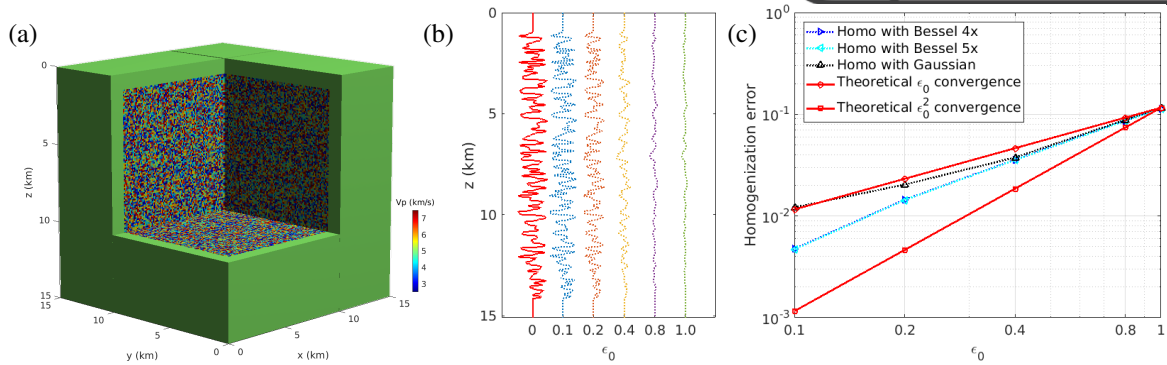


**Figure 3** Homogenization test in a random medium. (a) The random P-wave velocity model  $V_p$ , (b) 1D  $V_p$  profiles of the random model (red solid line) and the effective models using 4 Bessel filters with different  $\epsilon_0$  (dash lines), (c) the convergence history of the wavefields generated from the effective models with respect to  $\epsilon_0$  and the type of low-pass filters (Gaussian filter and its approximation through Bessel filters).

3b, we show the 1D depth profiles extracted in the middle of the resulting effective P-wave velocity ( $V_p$ ) models, with different scaling parameters  $\epsilon_0$  where  $\epsilon_0 = \lambda_0/\lambda_{min}$  with  $\lambda_{min}$  the minimum propagating wavelength depending on the medium property and the maximum frequency of the source  $f_{max}$ . In this test, we set  $\lambda_{min} = 800$  m, corresponding to the background S-wave velocity  $V_s = 3200$  m/s and  $f_{max} = 4$  Hz. Here  $\epsilon_0$  varies from 0.1 to 1.0 implying less and less small scales are kept in the homogenization. The homogenized wavefield solution is proved to converge asymptotically towards the reference wavefield solution (generated from the original medium) with a  $O(\epsilon_0^2)$  convergence (Capdeville et al., 2010). Figure 3c shows that we actually obtain a convergence order between  $O(\epsilon_0)$  to  $O(\epsilon_0^2)$  (see the dash lines between the two red lines). It is because the filter used to low-pass filter the concentrators has a wavenumber response slightly biased compared with an ideal boxcar-type filter considered in the optimal case. The feasibility of using a Bessel approximated Gaussian filter is confirmed by the good convergence agreement of the wavefield solution with the one obtained by convolving the true Gaussian-filter wavelet. The accuracy of the homogenized solution with an approximated Gaussian filter is even superior at low  $\epsilon_0$ , because its PDE-based implementation preserves the SEM precision consistency of all the steps in the homogenization.

The second example is based on a more realistic geological model: a 3D Marmousi-II model with a truncation of the water layer (the homogenization theory can not remove a fluid-solid interface, see Figure 4a). According to the same accuracy of homogenized solutions by using the cascade of 4x and 5x Bessel filters in the last example, here we adopt 4x Bessel filter to save computational costs. Figure 5 shows the projected anisotropic effective models to the nearest isotropic  $V_p$ ,  $V_s$  models and the remaining total anisotropy after the homogenization with scaling parameters  $\epsilon_0 = 0.2, 0.4, 0.8$ . As expected, we observe a significant apparent anisotropy behaving like a locally tilted transverse isotropy and its amount is increasing with  $\epsilon_0$  to compensate the small scale contrasts missing in  $V_p$  and  $V_s$  models. Since a variable coherent length can be used in the PDE-defined Bessel filter, our homogenization process is applied with a  $\lambda_0$  adaptive to the local minimum wavelengths instead of being constant, which makes it possible to use a constant  $\epsilon_0$  throughout the whole medium for providing a consistent asymptotic convergence from shallow to deep areas. Modelling tests induced by a vertical force with 2 Hz Ricker wavelet ( $f_{max} = 4$  Hz) are performed on these effective models and indicate a good agreement and convergence towards the reference solution with respect to  $\epsilon_0$ , as shown in the seismogram comparison in Figure 4b.

## Conclusions

We here explore the numerical implementation of non-periodic homogenization within a fully scalable parallel algorithm framework by applying domain decomposition parallelization and CG-based iterative method to its two main ingredients: solution of elastostatic equations and low-pass filtering. Since the conventional convolution-based Gaussian low-pass filtering is not compatible with the CG iterative scheme, we mimic the wavenumber response of the Gaussian filter with a cascade of elliptic PDE-defined Bessel filters that can be discretized by SEM and solved with a CG iterative method without any loss of effectiveness. In addition, this approximation makes good use of the variable coherent-length property of Bessel filter to adaptively remove the microscopic scales of the model on the basis of local minimum wavelengths. Two numerical tests in 3D validate the feasibility and effectiveness of the proposed parallel CG-based homogenization implementation, and indicate its high efficiency (more than half billion unknowns solved in less than 20 minutes, and scalability up around 1000 cores). All

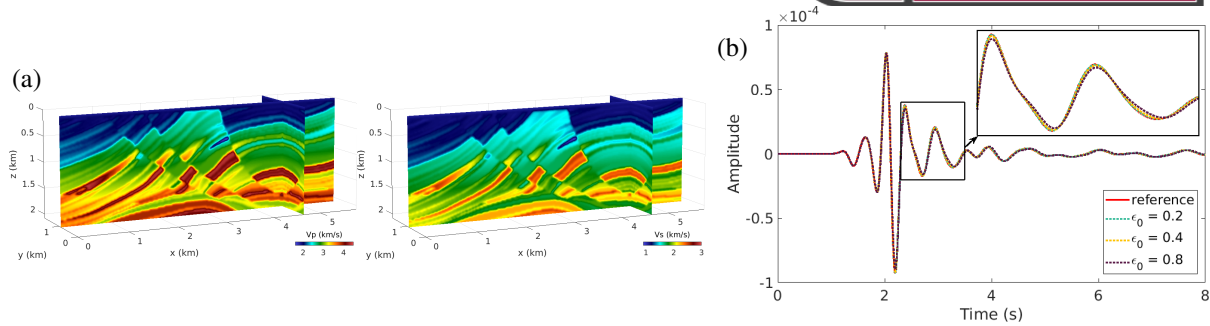


**Figure 4** (a) 3D Marmousi-II velocity models without the water layer which is used to calculate the reference solution for benchmarking against the homogenized solutions, (b) seismogram comparison of vertical displacement generated from (a) and the effective models with  $\epsilon_0 = 0.2, 0.4$  and  $0.8$  in Figure 5.

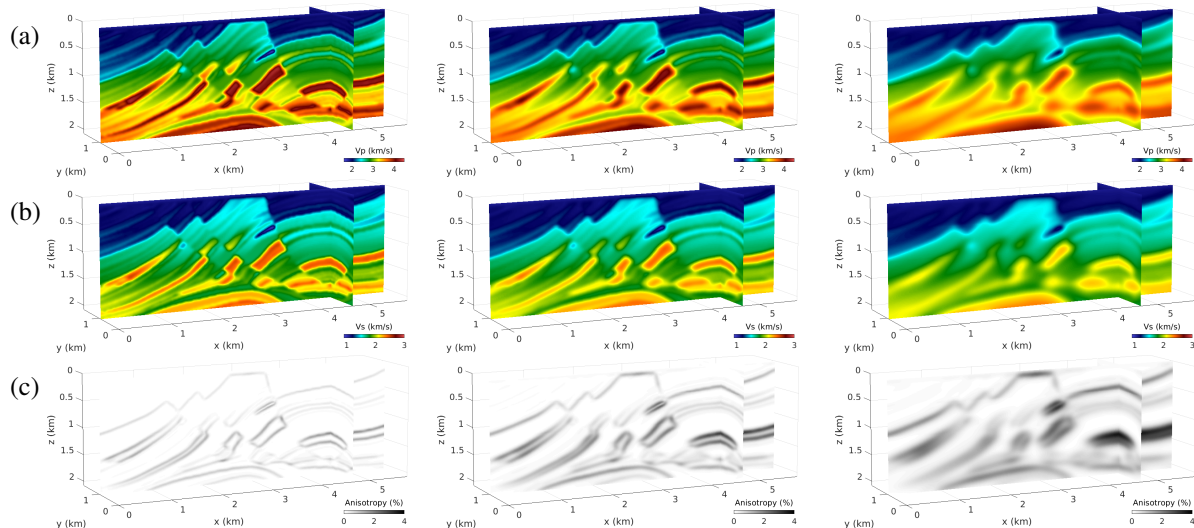


**Figure 5** 3D Marmousi-II effective models with  $\epsilon_0 = 0.2, 0.4$  and  $0.8$  from left to right. (a)  $P$ -wave velocity model ( $V_p$ ), (b)  $S$ -wave velocity model ( $V_s$ ) and (c) the total anisotropy in percentage, which are calculated by projecting the resulting  $C_{ijkl}$  from homogenization to the closest isotropic model (Browaeys and Chevrot, 2004).

these improvements make it possible to apply the homogenization process to large-scale industry-sized seismic full waveform modelling and inversion problems.

### Acknowledgements

This study was partially funded by the SEISCOPE consortium (<http://seiscope2.osug.fr>), sponsored by AKERBP, CGG, EXXON-MOBIL, GEOLINKS, JGI, PETROBRAS, SHELL, SINOPEC and TOTALENERGIES. This study was granted access to the HPC resources provided by the GRICAD infrastructure (<https://gricad.univ-grenoble-alpes.fr>), Cray Marketing Partner Network (<https://partners.cray.com>) and IDRIS/TGCC under the allocation 046091 made by GENCI.

### References

- Bensoussan, A., Lions, J. and Papanicolaou, G. [1978] *Asymptotic analysis of periodic structure*. North-Holland.
- Browaeys, J.T. and Chevrot, S. [2004] Decomposition of the elastic tensor and geophysical applications. *Geophysical Journal International*, **159**(2), 667–678.
- Capdeville, Y., Guillot, L. and Marigo, J.J. [2010] 2-D non-periodic homogenization to upscale elastic media for P-SV waves. *Geophysical Journal International*, **182**, 903–922.
- Capdeville, Y. and Métivier, L. [2018] Elastic full waveform inversion based on the homogenization method: theoretical framework and 2-D numerical illustrations. *Geophysical Journal International*, **213**(2), 1093–1112.
- Cupillard, P. and Capdeville, Y. [2018] Non-periodic homogenization of 3-D elastic media for the seismic wave equation. *Geophysical Journal International*, **213**(2), 983–1001.
- Hestenes, M.R. and Stiefel, E. [1952] Methods of conjugate gradient for solving linear systems. *Journal of Research of the National Bureau of Standards*, **49**, 409–436.
- Tang, J.H., Brossier, R. and Métivier, L. [2022] Fully scalable solver for frequency-domain visco-elastic wave equations in 3D heterogeneous media: a controllability approach. *Journal of Computational Physics*, **468**, 111514.
- Trinh, P.T., Brossier, R., Métivier, L., Virieux, J. and Wellington, P. [2017] Bessel smoothing filter for spectral element mesh. *Geophysical Journal International*, **209**(3), 1489–1512.